SINGS: The Spitzer Infrared Nearby Galaxies Survey
Second Data Delivery
April 2005

USER'S GUIDE

1. Introduction

This document describes the second data delivery of the Spitzer Legacy program SINGS. This is the first major data delivery from the SINGS team, and contains 1/3 of the total galaxies in the sample. The document is organized as follows: section 2 lists the data products contained in this delivery and their general characteristics; sections 3, 4, and 5 provide a description of the post-BCD processing for IRAC, MIPS, and IRS data, respectively; finally, section 6 briefly describes the data reduction steps of the ancillary data associated with this delivery.

For a complete description of the SINGS program, galaxy sample, and observing strategy, please refer to Kennicutt et al. 2003, PASP, 115, 928.

2. Content of the Data Delivery

2.1 Second-Delivery Sample and Data Products

The SINGS sample contains 75 galaxies, representative of a large range of properties of local normal galaxies (Kennicutt et al. 2003). Of these 75, 25 are in the present delivery (1/3 of the sample), and the full list of galaxies is given in Table 1. The 25 galaxies were chosen with the goal of providing a complete data coverage with IRAC, MIPS, and IRS.

Table 1: Galaxies in the SINGS second data delivery

Name	Name	Name
NGC0337	NGC3198	NGC4826
NGC1566	NGC3351	NGC5194
NGC1705	NGC3521	Tol89
HolmbergII	NGC3627	NGC5408
NGC2798	NGC3773	NGC7331
NGC2841	NGC3938	NGC7552
NGC2976	NGC4579	NGC7793
NGC3049	NGC4725	
NGC3190	NGC4736	

2.1.1 IRAC Mosaics

For each galaxy, 4 mosaics, one for each of the four IRAC bands, are delivered as single-extension FITS files. The pixel scale of the mosaics is 0.75 arcsec, and the flux scale is MJy sr^{-1}.

Details of the post-BCD processing are given in Section 3.

2.1.2 MIPS Mosaics

For each galaxy, 3 mosaics, one for each of the MIPS bands, are delivered as single-extension FITS files. The pixel scale of the MIPS mosaics is wavelength-dependent: 0.75 arcsec at 24 μm, 3.00 arcsec at 70 μm, and 6.00 arcsec at 160 μm. The flux scale is MJy sr^{-1}.

Details on the post-BCD processing are given in section 4.

2.1.3 IRS One-dimensional Spectra and Two-dimensional Images

Both Low-resolution and High-resolution, one-dimensional (1D) spectra of the central 23"x15" (High-res) to 50"x33" (Low-res) are delivered for each of the 25 galaxies, in the wavelength range 5-15 μm (Short-Low, SL, R=50-100), 15-37 μm (Long-Low, LL, R=50-100), 10-20 μm (Short-High, SH, R=600), 20-37 μm (Long-High, LH, R=600). The fluxes are calibrated in MJy sr^{-1}. The data are provided as multiple ASCII files (.tbl).

Two-dimensional continuum-subtracted line maps in [SiII] 34.8μm, and [NeIII] 15.5 μm (where available), and maps of poly-cyclic aromatic hydrocarbon emission (7.6μm+8.6μm, 11.3μm), are also delivered for the 25 galaxies, plus the adjacent continuum maps at 15μm and 35μm for the emission lines. The images are delivered as single extension FITS files. The units of the [NeIII] and [SiII] line maps are W m^{-2} sr^{-1}, while all other maps have units MJy/sr.

Details on the data format and content, and on the post-BCD processing for the spectra are given in section 5.

2.1.4 Optical Images/Mosaics

Optical imaging data in the standard B, V, R, I broad-band filters and in narrow-band filters at the wavelength of the Hα+[NII] emission, plus continuum-subtracted Hα+[NII] images, are delivered for 24 of the 25 galaxies (for NGC5408, only the continuum-subtracted Hα and associated continuum images are available).

The images are either single pointings, or mosaics of 2 or more adjacent and partially-overlapping frames. **T**he images are not background-subtracted.

All optical data are single extension FITS files (one file for each filter); they are flux calibrated and have astrometric solutions. Photometric and astrometric keywords are stored in the FITS headers.

The pixel scale is 0.305 arcsec (KPNO data) or 0.433 arcsec (CTIO data). The images have NE orientation, and are registered to a common frame. The flux scale is count/sec (CPS), and the relevant photometric keywords are: PHOTFLAM, to convert CPS to Jy, and ZPOINT, for the zeropoint.

More details on the optical images are given in section 6.1.

2.1.5 Optical One-dimensional Spectra

One-dimensional (1D) spectra in the wavelength range 0.36-0.70 μm are delivered for 22 of the 25 galaxies (there are no spectroscopic data available for HolmbergII, NGC5408, and NGC7552). For most galaxies, two spectra are delivered: the nuclear spectrum and the central 20”x20” drift-scan spectrum. For NGC2976 and Tol89 only the central 20”x20” drift-scan spectrum is available.

The nuclear spectra are 2.5”x2.5” (KPNO) or 2.5”x3.0” (CTIO) aperture extractions of the brightest few central pixels. The 20”x20” drift-scan spectra target the central region of each galaxy, in a similar fashion to some of the IRS spectra. Both type of optical spectra are wavelength and flux calibrated. Resolution is ~8 Angstrom, and all fluxes are corrected for foreground Galactic extinction.

Nuclear and drift scan spectra are stored in separate ASCII files (*.txt). More details on the data are given in section 6.2.

2.2 File Name Convention

For each galaxy, multiple datasets are delivered, with the following filename convention:

- *IRAC mosaics*: ngcXXXX_v4_irac#.fits (with #=1,2,3,4; e.g., ngc0337_v4_irac1.fits)
- *MIPS mosaics*: ngcXXXX_mips#.fits (with #=24,70,160; e.g., ngc0337_mips24.fits)
- *IRS Low-Res 1D spectra*: ngcXXXX_DR2_MD#_nuc_sp.tbl (MD=SL,LL; #=1,2)
- *IRS Low-Res 1D Estimated Background Spectra (selected sources only):* ngcXXXX_DR2_SL#sky_sp.tbl (#=1,2)
- *IRS High-Res 1D spectra*: ngcXXXX_DR2_MD_nuc_sp.tbl (MD=SH,LH)
- *IRS 2D Maps*: ngcXXXX_DR2_MD#_line.fits (line=neIII, siII, pah_8, pah_11_3) and ngcXXXX_DR2_MD#_line_cont.fits (line=neIII, siII)
- *Optical images/mosaics*: ngcXXXX_#.fits (with #=B,V,R,I,Hα,Hα_sub e.g., ngc5194_Ha.fits)
- *Optical 1D spectra*: ngcXXXX_nuclear_002_5.txt and ngcXXXX_drift_020_020.txt.

3. IRAC Data Products and Post-BCD Processing

3.1 Introduction

The SINGS IRAC images are created from multiple Spitzer images in either a mosaic or single field dither pattern. The fundamental data used for these are the Version 11 Basic Calibrated Data (BCD) images produced by the Spitzer Science Center (SSC). These data have already undergone a number of processing steps including conversion from engineering to scientific units, flat fielding and bias subtraction. The SINGS IRAC pipeline further processes these data to deal with a number of issues including frame geometric distortion and rotation, residual flat fielding, cosmic rays, frame alignment, and bias drift. Frames are finally combined using the drizzle algorithm to maximize resolution from the individual sub-sampled images. The major observation and processing steps are detailed below.

3.2 Data Products

The IRAC data products contained in this delivery are single-extension FITS files, one file for each IRAC band (*.irac1.fits, *.irac2.fits, etc.). The images are calibrated in MJy sr^{-1}, and have pixel size of 0.75 arcsec.

The original header keywords are retained, plus others added as a result of the post-BCD processing. In particular, astrometry is stored using FITS standard WCS coordinate keywords; the flux scale is stored in the BUNIT keyword; and the background subtraction and its value are stored in the keywords BACK_SUB (performed=T, not performed=F) and BACKGRND (value), respectively.

3.3 Observational Strategy

Observations were carried out in accordance with the SINGS IRAC observing strategy (Kennicutt et al. 2003). For galaxies larger than the 5' size of the IRAC detectors, observations are taken in a mosaic pattern, offsetting the field of view by ~50% each time. This process is repeated twice, with observations separated by at least 24 hours to best correct for asteroids and detector artifacts. Points in the central mosaic regions are thus imaged eight times and the outermost regions four times. Galaxies fitting in a single IRAC field are imaged using two sets of four dithered observations, again resulting in points being observed eight times over the bulk of the final images. Observations are 30 seconds in duration with an additional one second exposure taken at each pointing to provide data in cases where the main observation is saturated.

3.4 Image Processing

The steps performed by the SINGS IRAC pipeline are the following:

a. Geometric Distortion and Image Rotation

BCD images contain geometric distortions caused by IRAC's off-axis location in the Spitzer focal plane. The magnitude of these distortions is up to 2.2". These are corrected for in the SINGS IRAC pipeline using coefficient tables obtained from the GOODS team. Frames (single-exposure images) from the second set of exposures are also rotated to the

orientation of the first using the header position angle difference between the first images of each observation set.

b. Bias Structure

At present there is some residual bias structure in the IRAC BCD data, particularly affecting band 3. To address this issue, IRAC band 3 frames for galaxies observed with a mosaic pattern are median combined and the result subtracted from each frame. This method is not applied to observations obtained with a dither pattern (small galaxies), as in this case the object occupies a large fraction of each frame, thus strongly affecting the median.

c. Image Offsets

Offsets between individual BCD images are determined through image cross-correlation. In this process, rough cosmic ray rejection is first carried out by comparing the short and long IRAC exposures at each pointing. Geometric distortion corrections are also applied. Any two frames with at least 10,000 pixels in common are cross-correlated with each other. Individual frame pair cross-correlation results from all four bands are combined for maximal accuracy, weighting offsets by their errors and applying outlier rejection. Within each band, a consistent solution for frame positions is then obtained through least square fitting. Accuracy for this process varies from galaxy to galaxy, but is generally in the range 0.1-0.2 pixels.

d. Bias Drift

IRAC images are at present still subject to full frame DC bias drift with time. To correct for this, the SINGS IRAC pipeline matches the median flux level in regions of overlap and determines any DC offset between overlapping frames. This offset is assumed to be due to the bias drift. χ^2 minimization is again applied to find a consistent solution for all frames and the appropriate DC offsets applied. It should therefore be noted that a small unphysical offset may be present in the SINGS IRAC images.

e. Cosmic Rays

Final cosmic ray masks are created using standard drizzle methods (see the HST Dither Handbook: http://www.stsci.edu/instruments/wfpc2/Wfpc2_driz/dither_handbook.html). Each image is first drizzled to correct for geometric distortion. The weight files from this step are also used to create pixel masks. Following this, the images are median combined to reject cosmic rays. These images are then 'blotted' - a step that effectively reverses the steps so far - to create images equivalent to the original input images but without cosmic rays. Finally, a spatial derivative is calculated to assess the effects of blurring in the median image (Dither Handbook, page 60) and the original and blotted images are compared to obtain a cosmic ray mask for each image.

f. Final Images

The final step in the SINGS IRAC pipeline is to drizzle the original long exposures together, applying the geometric distortion and rotation corrections, cosmic ray masks and determined image offsets. In this process, the output pixels are scaled to 0.75 arcsec. A drop-size of 0.75 input pixels is applied. These values are chosen to yield fully

sampled images with maximal resolution. A correction factor is also applied to the final images to maintain accurate photometry given the change in pixel size. Blank pixels in the final mosaic images are set to IEEE NaN (not a number).

The final drizzle step combines together the images from the two different AORs, thus removing asteroids in the process.

3.5 Known Problems and Image Artifacts

In using the final images, users should be aware that at present the astrometry between bands has not been made fully consistent. As such, there may exist small offsets in object world coordinates between bands, typically less than 1 pixel (0.75”), with occasional peaks of 2 pixels.

Also, as mentioned earlier, small background level corrections have been applied to individual frames to correct for bias drift, potentially leading to an unphysical offset in the final images (i.e., slightly negative backgrounds). For galaxies observed with a single dithered pointing (NGC0337, NGC1705, NGC2798, NGC3049, NGC3773, Tol89, NGC5408, and NGC7552), the bias drift correction (section 3.4, point d) cannot be properly applied. As such, the off-target image can have a background level which is different from that of the on-target image (by up to 1 MJy/sr). This is also true for NGC2841 which does not have sufficient overlap between the south and north parts of the image for this correction to be applied.

Users should be aware that images in this delivery are generally not background subtracted, with the exception of large, mosaiced galaxies in band 3, which have had a background component removed as part of the bias structure median correction process. The details of any background subtraction are given in the BACK_SUB and BACKGRND header keywords.

A number of band 3 and 4 images show a persistent gradient in the background, which results in changes by (typically) up to 0.1 MJy/sr in the level between one side of the image and the other. Processing fixes are being considered for future deliveries to further alleviate BCD bias problems.

No aperture corrections have been applied to the final data products. IRAC calibrations are performed using a 12” radius aperture on stars, and corrections need to be applied for photometry at other aperture sizes or for photometry of extended sources. Correction factors are given in the Infrared Array Data Handbook, Version 1.0, p39.

Finally, users are cautioned to be aware of standard IRAC detector artifacts that may also be present in the SINGS data. These are detailed extensively elsewhere (Hora et al. 2004, SPIE, in press; Fazio et al. 2004, ApJS 154, 10) and include: persistent images in channels 1 and 4, diffuse stray light, stray light from point sources, Muxbleed, column pulldown and banding, remaining full-frame bias and ghost images. Because we combine two epochs of observations that are slightly rotated and we match the backgrounds between overlapping BCD images, some of the detector anomalies are mitigated in our final mosaics.

3.6 Notes on Individual Galaxies

NGC 2841: In the channel 3 image of this galaxy, a background gradient of 0.6 MJy/sr between the North and South sides is present. The overlap between individual mosaic pointings in this galaxy is not large enough for the bias drift step in the SINGS IRAC pipeline to work properly (section 3.4, point d).

NGC3198: The channel 3 image of this galaxy shows a `saddle-shaped' background, with a negative variation of 0.1 MJy/sr at the center relative to the edges.

NGC 4725: A smaller cross-correlation image overlap requirement of 1,000 pixels was found necessary in processing this galaxy.

NGC 5408: Mosaics contain some very bright foreground stars. The centers of some of these have been rejected in the Band 1 image by the cosmic ray flagging routine.

NGC7552: In Band 4, scale factors 7 times larger that standard were used in the cosmic ray rejection steps to minimize the number of pixels rejected in regions heavily affected by Muxbleed.

4. MIPS Data Products and Post-BCD Processing

4.1 Introduction

The SINGS MIPS mosaics in this delivery were created from multiple Spitzer images obtained in scan-mapping mode, and fully processed with the MIPS Data Analysis Tool (MIPS DAT, Gordon et al. 2005, PASP, in press, http://mips.as.arizona.edu/mipspage/dat.pdf). The major observation and processing steps are detailed below.

4.2 Data Products

The MIPS data products contained in this delivery are single-extension FITS files, one file for each MIPS band (*_mips24.fits, *_mips70.fits, and *_mips160.fits). The images are calibrated in MJy sr^{-1}, and have pixel size 0.75, 3.00 and 6.00 arcsec for the 24 μm, 70 μm, and 160 μm mosaics, respectively. The pixel sizes of the MIPS mosaics have been chosen to adequately sample the point spread function and at the same time be an integer multiple of the IRAC mosaics' pixel scale (approximately 0.75 arcsec, see section 3). Backgrounds have been subtracted from the data as part of the data processing.

All original fits header information has been retained. The headers' content has been re-arranged so that basic information on the observations, the target, and coordinates, and the pixel sizes appears first in the listing. Among the relevant keywords: the mosaics' astrometry is stored in the standard FITS WCS keywords; the flux units are stored in ZUNITS; and, as for the IRAC images, the background subtraction and its value are stored in the keywords BACK_SUB (performed=T, not performed=F) and BACKGRND (value), respectively. (Note that the BACKGRND keyword is missing in some fits files because of a problem with creating the header information.) All other information, which includes details on the observations and the data processing, is located after these basic keywords.

4.3 Observational Strategy

The MIPS observations were obtained using the scan-mapping mode in two separate visits to the galaxy. Separate visits allow asteroids to be recognized and provide observations at orientations up to a few degrees apart to ease removal of detector artifacts. As a result of redundancy inherent in the scan-mapping mode, each pixel in the core map area was effectively observed 40, 20, and 4 times at 24, 70, and 160 microns, respectively, resulting in integration times per pixel of 160 s, 80 s, and 16 s, respectively.

4.4 Post-BCD Image Processing

The MIPS data were processed using the MIPS DAT versions 2.80 – 2.96 along with additional customized processing software. The processing steps are as follows.

1. For the 70 and 160 μm data, a linear fit is applied to the ramps (the counts accumulated in each pixel during the non-destructive readouts), and slopes are derived. This step also removes cosmic rays and readout jumps. An electronic nonlinearity

correction has also been applied to data processed after the correction was available in this step of the data processing.

2. The initial processing of the 24 μm data is different from the 70 and 160 μm data, as the 24 μm data are received as already containing the slopes fitted to the ramps. Thus, the 24 μm images are processed through a droop correction (that removes an excess signal in each pixel that is proportional to the signal in the entire array), correction for non-linearity in the ramps, and dark current subtraction. In some data, a rowdroop correction (which corrects a droop effect only visible along the rows of the detector) was applied, but it should be noted that a software bug limited the accuracy of the rowdroop correction. This can have a small (< 1%) effect on a single detector row that crosses a saturating source.

3. Telescope optical signatures and time-dependent responsivity variations in the detector elements are removed from the data, in the following way:

a. For the 24 μm images, scan-mirror-position dependent and independent flatfields are applied to the data in two steps. First, scan mirror position dependent flatfields are applied to the data. These flatfield either are created from off-target data in all SINGS scan maps from a given campaign or are selected from a library of flatfields created by the MIPS instrument team. Next, scan mirror position independent flats are created from off-target data; these flatfields are applied to the data to remove any residuals left by the scan-mirror-dependent flats. In some data, a readout offset correction is applied between the flatfielding steps to correct a "jailbar" effect that is seen in images with highly saturating sources. Latent images in the 24 μm data are masked out after the flatfielding.

b. The stim flash frames taken by the telescope are used for responsivity corrections of the 70 and 160 μm arrays. Next, the dark current is subtracted, and illumination corrections are applied to the data. Following this, short-term variations in the images caused by drift are subtracted. This last step also subtracts the background from the data.

c. After these data processing steps, the individual data frames are visually and statistically inspected for erroneously high or low pixel values and bad frames. Any such data that are found are set to NaN for further data processing.

d. In some data, an additional step is performed on the 24 micron data in which the background is subtracted from the individual frames. This is done by finding the background levels as a function of time for each individual scan leg while excluding the target, then fitting a third order polynomial to the background values. The function is then used to calculate the background for each frame, and this background is subtracted.

4. Final mosaics are made from the individual frames. Note that,

a. In all 70 and 160 μm data as well as all 24 μm data with background subtraction in individual scan legs, data fom both AORs are mosaiced together. After this step, backgrounds are subtracted from the data in all wavebands using the following methods:

i. Backgrounds in the 24 μm data are measured in multiple small circular regions specifically chosen by eye near the optical disk to avoid bright background or foreground sources.

ii. Backgrounds in the 70 and 160 micron images are measured in two or more regions that straddle the target. These regions cover an area at least twice as large as the galaxy. They are chosen by eye so as to match the background region under the target itself and to avoid bright sources. These background values are then subtracted from the final map. Since the short-term drift removal does subtract most of the background, this step removes only a residual offset.

b. In 24 μm data without the background subtraction in individual scan legs, the 24 μm data from each AOR are mosaiced separately. After mosaicing, backgrounds are subtracted from the two 24 μm images in two steps. First, planes ($z=Ax+By+C$) are fit to the background counts inside square regions centered on the galaxy and with size three times the galactic optical diameter. Pixels within the optical disk of the galaxy are excluded from the fit. After the fitting planes are subtracted, any residual offset is measured in regions near the optical disk and subtracted. The two mosaics are then averaged together to make a final 24 μm mosaic.

5. After the mosaics are created, the images are multiplied by a final calibration factor that converts the MIPS units into MJy sr^{-1}. The calibration factors are derived after all processing steps have been applied to the mosaics. The factors are the following (keyword JANSCALE in the image headers):

24 μm: 0.0439 MJy sr^{-1} $MIPS\_units^{-1}$

70 μm: 634 MJy sr^{-1} $MIPS\_units^{-1}$

160 μm: 42.6 MJy sr^{-1} $MIPS\_units^{-1}$

The *mosaics in this delivery have been cropped* to sizes that include all of the galaxies' optical disks and any nearby galaxy or extended structure. The cropped images also include a minimum of 40" space between the edge of the optical disk and the edge of the image, so that sufficient information for measuring the background is provided.

4.5 Known Problems and Uncertainties

Streaking in the 70 μm data

Bright sources in the 70 μm data produce negative latent images that are manifested as negative streaks in the data. Sometimes positive streaks on the opposite side of the bright sources from the negative streaks are also apparent. These positive streaks are regions where, partly because of the negative latent images, the background is undersubtracted. Work is underway to correct the negative streaking, which should also lead to a reduction of the positive streaking.

In the current delivery, the following galaxies have the most severely `streak-affected' 70 μm images: NGC2798, NGC3351, NGC3521, NGC3627, NGC4736, NGC4826, NGC7552.

Artifacts near Bright Sources in the 24 μm data

In some cases, sources in the 24 μm data trigger a strong "jailbar" effect and a droop effect visible as a step function in the background. Work is underway to properly correct both of these effects.

In the current delivery, the only galaxy affected by this problem (on target) is NGC7552.

Photometric Uncertainties

Currently the estimated calibration uncertainties for MIPS extended object photometry are ~10% for the 24 μm data and ~20% for the 70 and 160 μm data.

5. IRS Data Products and Post-BCD Processing

5.1 Observations and Data Products

The IRS data products provided in this second data release consist of i) a representative nuclear spectrum in each of the four IRS modules — Short-Low (SL, 5-15 μm, R=50-100), Long-Low (LL, 15-37μm, R=50-100), Short-High (SH, 10-20μm, R=600), and Long-High (LH, 20-37μm, R=600), ii) continuum-subtracted line maps in [SiII] 34.8μm, and [NeIII] 15.5 μm (where available), iii) complementary continuum maps at 15μm and 35μm, and iv) maps of poly-cyclic aromatic hydrocarbon emission (7.6μm+8.6μm, 11.3μm).

All SINGS IRS observations are taken in the Spectral Mapping Mode, in which the slit is moved in a raster pattern to build up a redundantly-sampled spectral map of the target region. For this release, we are providing extractions of a rectangular region ranging in size from 22.6″×14.8″ (high resolution, SH and LH) to 50″×33″ (low resolution, SL and LL), centered on the nucleus of each galaxy. An example illustrating these extraction regions overlaid on the 8μm image of M51 is shown in Fig. 1.

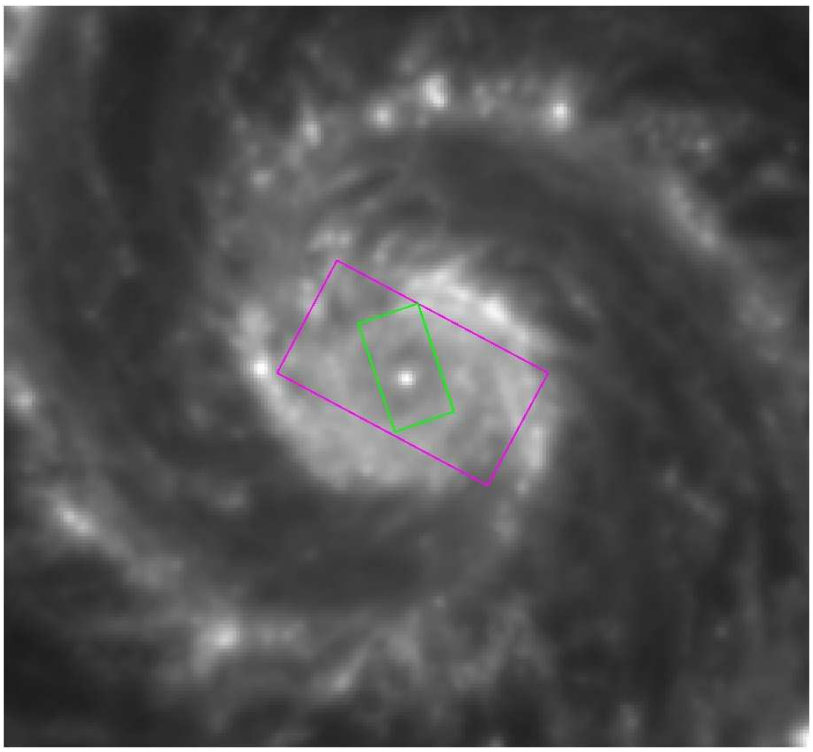

Figure 1: The 8μm image of M51, with example extraction regions for the IRS spectra in this delivery, shown with the following overlays: magenta: low resolution nuclear spectra, green: high resolution nuclear spectra.

5.2 File Format and Naming Convention

All spectra are formatted as ASCII files in the IPAC table format. The brief headers give the date of each observation, corresponding to the first data collection event in the spectral map, as well as the location of the regions over which the data were extracted.

Low-Resolution Spectra are divided by module and order, with the naming convention:

ngcXXXX_DR2_MD#_nuc_sp.tbl

where "md" is the module (SL, LL), "#" is the order (1 or 2). Each file consists of a header followed by the data in two columns: wavelength (in μm), and flux intensity (in MJy/sr). For those sources listed as "Model 1D" in Table 2, second column, SL1 and SL2 estimated background spectra are provided, with names ngcXXXX_DR2_SL#sky_sp.tbl.

High-Resolution spectra are also divided by module, with the naming convention

ngcXXXX_ DR2_MD_nuc_sp.tbl

where "md" is the module, either "SH" or "LH". Each file consists of a header followed by the data in two columns: wavelength (in μm), and flux intensity (in MJy/sr). Data from overlapping orders are interpolated and averaged in each high-resolution spectrum.

All maps are formatted as FITS files with header information describing the wavelength range of foreground and continuum regions used to construct the map. The maps are labeled

ngcXXXX_DR2_MD#_{neIII,siII,pah_8,pah_11_3}.fits

where neIII, siII are the continuum subtracted neon and silicon line maps, the pah_8 and pah_11_3 are the 7.6μm+8.6μm and11.3μm maps respectively. The associated continuum maps are labeled

ngcXXXX_DR2_MD#_{neIII,siII}_cont.fits

Note that the units of [NeIII] and [SiII] line maps are W m^{-2} sr^{-1}, while all other maps and spectra have units MJy/sr. Examples of some of these products are shown in Figure 2.

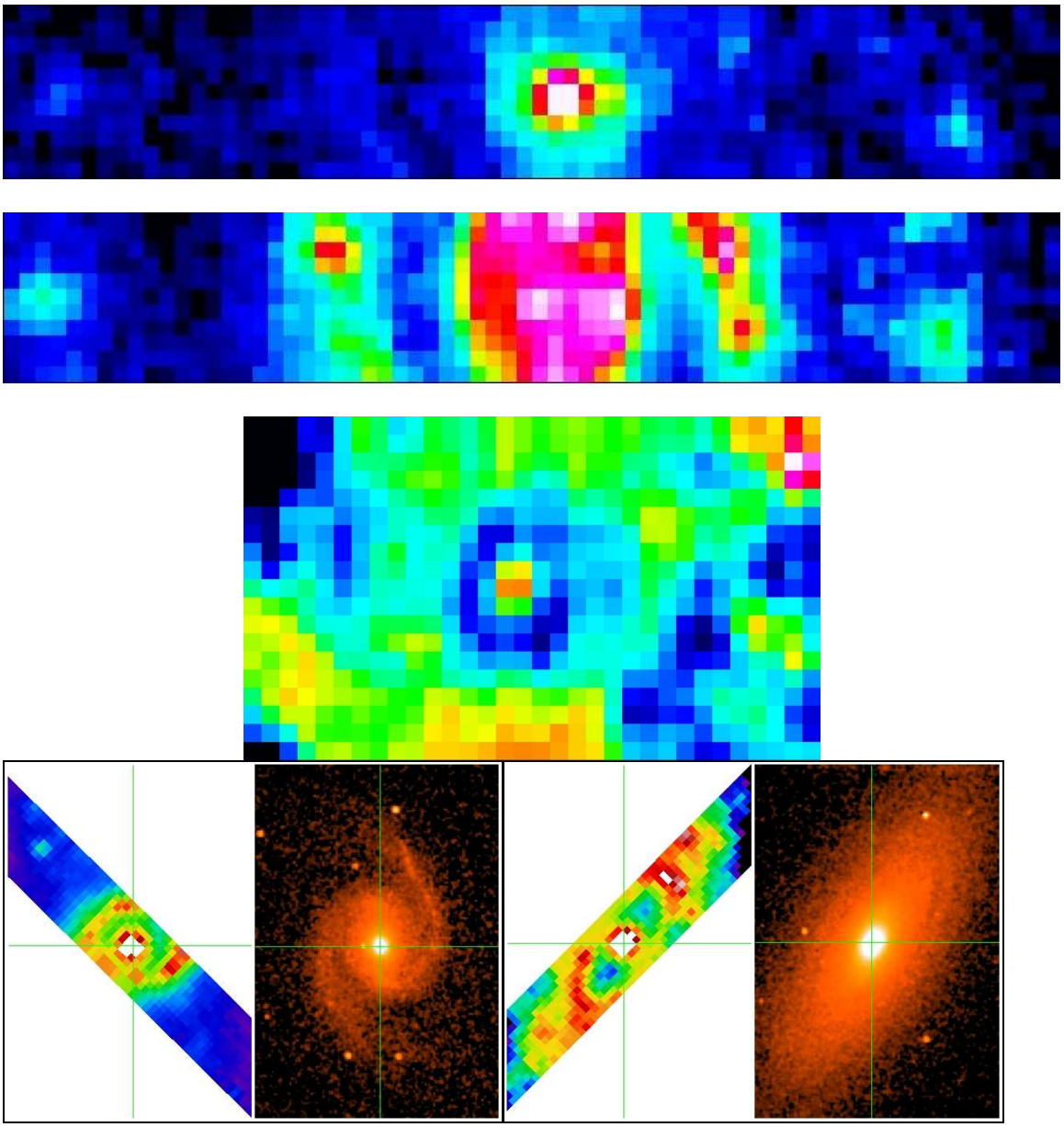

Figure 2. Top 3 panels are examples of DR2 products for NGC 5194. Top panel is the central portion of the continuum-subtracted [NeIII] emission. It is highly centrally concentrated compared to the continuum-subtracted [SiII] emission, shown in the second panel; it shows bright emission in the nucleus and the spiral arms. The third panel shows the integrated PAH emission at 8μm. The fourth and fifth panels show a side-by-side comparison of a 2MASS K-band image and a LL1 map for NGC 1566 and NGC 2841 respectively. The IRS maps have very good astrometry, typically within 1" of the 2MASS coordinates, as indicated by the cross airs in the last two panels.

5.3 Data Processing & Mapping

Low-Resolution Products

The low resolution spectral mapping data were assembled into three-dimensional spectral cubes using Cubism, a tool specifically designed for this purpose (see Kennicutt et al, 2003, Sect. 6.2, for more information). Bad pixels are flagged and removed in situ in the redundantly sampled map (typically 10-50 per frame). Background subtraction and flux calibration (described in more detail below) are performed on each cube.

Maps of the nuclear regions are made by averaging the cube along the wavelength dimension over the extraction regions noted above. Line maps are made by continuum-subtracting and integrating the cube over a suitably redshifted wavelength range for the line or feature. The continuum is estimated using a weighted average of nearby continuum values, with weight that varies inversely with the wavelength offset.

A matched rectangular region of 30″×52″ was used to extract the low-resolution spectra. (An exception is for NGC7331, our validation galaxy, for which a smaller SL map was obtained, yielding a smaller extraction regions of 15″×52″). Non-calibrated data at the ends of orders are trimmed for the final spectrum.

High-Resolution Products

High resolution maps were also created with Cubism. Time varying bad pixels, which respond to light, but vary on timescales of days to weeks, dominate the noise in the high-resolution spectra, LH in particular. These pixels were manually flagged, typically numbering 100-200 in SH and 200-400 in LH, and are rejected from the extraction. In all cases, noisy areas at the red and blue ends of each spectral order have been trimmed to create the final, fully stitched SH or LH spectrum. The low- and high-resolution apertures are not the same size, and their relative orientation depends on the exact dates of the observations.

A matched aperture for the full size of the 3×5 SH map, roughly 23″×15″, was used for both high-resolution extractions. Note that the low- and high-resolution apertures are not the same size, and when the low and high resolution observations are done of different days, their relative orientations is different depending on the telescope roll angle.

Sky or Background (and Foreground) Subtraction

The sky emission is estimated or taken directly from the maps, and subtracted from all low-resolution maps and spectra. No sky emission was removed from the high-resolution spectra; estimating equivalent widths or other continuum-sensitive measures in high-resolution spectra will require the use of an estimated background spectrum, available in Spot.

LL: The LL maps, assembled from long radial strips which extend 10' or more across the galaxy, contain a robust measure of the nearby zodiacal and cirrus "background" (which actually is mostly foreground emission). Typically 10-30 spectral frames were averaged together with min/max trimming for subtraction in the 2D spectral image. This process not only removes the background, but also restores many of the time-varying bad pixels to the proper scale.

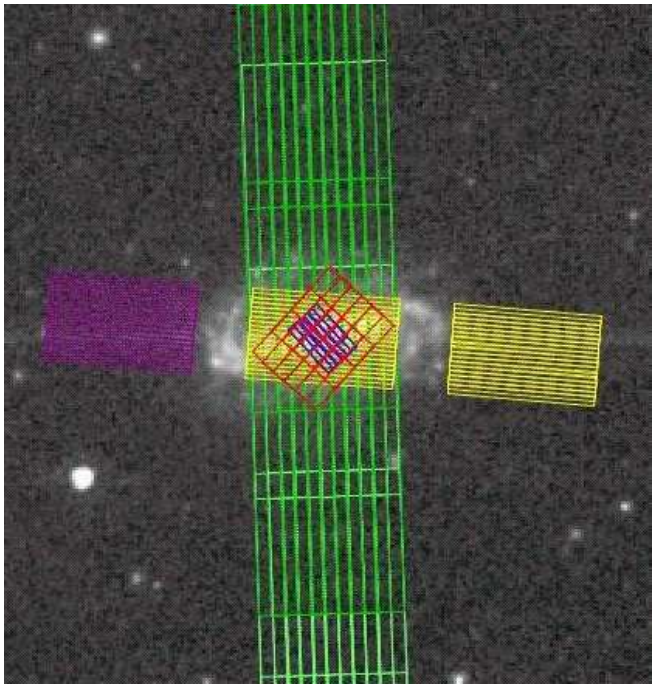

Figure 3: An overlay of the IRS observations on NGC 3049. Notice how the “outrigger” SL2 and SL1 observations serve as a short-low background for this small galaxy. The LL background is determined from the LL BCDs at the ends of the radial strip.

SL: Unlike the LL maps, the SL maps are much smaller, and the background cannot always be measured using the outermost portions of the maps. However, for small galaxies, the areas mapped by the outrigger order may be used for background subtraction. An example where an outrigger map may be used for sky estimation is NGC3049, as shown in Figure 3. This method of using SL outrigger data for sky subtraction was possible for 10 of the 25 galaxies in this release (see Table 2). For another 5 galaxies in this release we obtained dedicated off-galaxy sky observations (labeled "Dedicated" in Table 2). For the remaining 10 galaxies in this release, our approach to SL sky subtraction is outlined below.

We identified 27 galaxies from the entire SINGS sample for which SL sky spectra can be extracted using either outrigger or dedicated sky observations. For galaxies without outrigger or dedicated background spectra, we interpolated the sky spectrum from the suite of outrigger and dedicated background data obtained for other galaxies. The key to this scheme is the interpolating parameter. In general, the shape and amplitude of the background spectrum over SL wavelengths can be parameterized by the 24 μm flux. The parameterization works well using the 24μm background flux from either MIPS imaging or the predictions from Bill Reach's models (2003, available via SPOT); we employ the latter.

In practice, polynomials are fit to each 1D sky spectrum. To generate a 1D background estimate spectrum for galaxies without outrigger and dedicated sky observations, we interpolate amongst the suite of polynomial fits using the 24 μm flux as the interpolating value.

Thus we constructed 1D estimates of the SL sky for 10 of the 25 galaxies in this release (Holmberg II, n3521, n4725, n4736, n5194, n2841, n2976, n3198, n3627, n393).

Flux Calibration

The flux calibration in the SSC pipeline is optimized for point sources. For these, the extraction aperture is an expanding aperture chosen to minimize jumps between orders and modules induced by varying fractions of the point spread function. The extracted spectra are trimmed at the ends of orders and fit to a stellar models using a low-order polynomial. For extended sources, however, an expanding aperture is inappropriate since the emission fills the slit. Moreover, the implicit correction for light losses as a function of wavelength, that are applied as a part of the calibration for a point source, need to be *removed* for an extended source. The former correction is referred to as an aperture loss correction function (ALCF) and the latter is referred to as a slit loss correction function (SLCF). We employ an ALCF implicitly by deriving a new flux calibration for well-modeled standard stars using a large 24 pixel (non-expanding) extraction aperture. We estimate the SLCF for the low-resolution modules using a theoretical model of the slit width and instrumental PSF, as discussed in Sloan (2004). The SLCF is an exact correction only for perfectly uniform extended sources. Though SINGS sources span a full range of structure, we have applied the same uniform slit loss correction to all sources.

To estimate the unknown effective pixel solid angles (which relate to the integral across the slit of the beam profile), we employed matched photometry using our MIPS and IRAC maps. We compared the imaging and spectral photometry at 5.7μm (SL2 vs. IRAC3), 8μm (SL1+SL2 vs. IRAC4), and 24μm (LL1 vs. MIPS24). We applied the imaging filter transmission curves to the extracted IRS spectra and compared the simulated broad band fluxes to the observed fluxes from the IRAC and MIPS images over the same region in all the galaxies; we used the results of these comparisons to derive the effective cube pixel solid angle. For LL, the results converged on a value very near the empirically measured slit width. For SL, the uncorrected photometry indicated an effective pixel solid angle that resulted in the SL spectrum overlying the LL significantly, and implied an effective pixel solid angle less than the measured slit width. There are more than one possible reasons for this discrepancy. One possibility is the variable extended source correction that is inherent to some IRAC bands[1], which results in derived fluxes at 8μm that are too high. An IRAC4 correction factor is not available over the intermediate scales covered by our low-resolution extraction regions, but is roughly figured to be a downward correction between 10% and 40%. To estimate the true SL effective pixel solid angle, we use the overlap with LL at 15μm, and found good agreement with the expected offset implied by the IRAC corrections. The second possibility is an uncertainty in the Slit Loss Correction Factor, as it is not known a priori whether the source is truly extended and with a flat spectral energy distribution.

Since we have not attempted to remove the background from the high-resolution spectra, they have in general a much higher continuum fluxes than low-resolution spectra extracted nearby. Users are urged to estimate the background using the Reach et al. (2003) available in Spot. The high resolution spectra also were not treated with a slit loss correction function, which could translate to structure-dependent correction up to ~10%, and which would tend to *lower* the implied fluxes.

Effective Integration Times

All spectra delivered are the composite of multiple exposures. For the high resolution results, 30 (15) individual DCE's totaling 15.73 min (15.24 min) of integration time were combined to produce a single SH (LH) spectrum. For SL spectra, the full maps required only 8.8 min (4.4 min each for SL1 and SL2), and the majority of the on order data were averaged together to produce the spectrum. The much larger LL strip maps ranged from 20.97 min to 41.95 min total integration time. The effective integration times per pixel were 58.7 sec in SL, and 125.84 sec in LL. Only 4-7% of the full LL map was used to match the SL extraction region, although 10-20% of the map (taken from the extremities) was also used for background subtraction.

[1] See http://ssc.spitzer.caltech.edu/ost/workshop/2005data/talks/carey2.pdf

For a given peak source flux, the signal-to-noise in the resulting spectra depends critically on the spatial distribution of the source. For galaxies with significant extended emission in the extraction regions (e.g. NGC5194), the relative S/N achieved is much higher than for galaxies whose mid-infrared flux is concentrated in the nucleus (e.g. NGC5408). In many cases, higher S/N spectra could be achieved by extracting over smaller regions; for consistency all regions were chosen to be the same size.

5.4 Data Artifacts and Known Problems

Spectral Mismatch and Astrometric Uncertainty

The 4 segments of the low-resolution spectra (SL2, SL1, LL2, LL1, in order of increasing wavelength) are derived from separate spectral cubes with individual astrometry. Astrometric errors typically of order 1.5" can contribute to a mismatch between SL and LL, and, to a lesser degree, to mismatch between orders in the same spectral module (SL1 and SL2, LL1 and LL2). Also contributing to the mismatch is the unknown aperture correction that is assumed by the SLCF which has assumed a smooth source brightness distribution.

Extended Source Flux Calibration

As noted above, we are developing a calibration strategy for extended sources in conjunction with the SSC. All low resolution spectra have been treated with an approximate extended source slit correction; the residual systematic error in these spectra is 15%. While the high resolution data do not need an extraction aperture correction, they do need a slit correction function applied; these functions are not yet determined for SH and LH. The correction is anticipated to be largest at the wavelength at which SH and LH meet (~20μm). The estimated systematic uncertainty which results from not applying this correction is 30%. This uncertainty will be important when, e.g., estimating line flux ratios for lines which span both the SH and LH modules.

Flux Conversion Errors

In DR1 we noted an error in the flux conversion tables (FLUXCON) specific to the pipeline version of the processed raw data used for that delivery (version S10.5a). This problem has been mitigated in S11.

Residual Time-Varying Pixels

Responsive, yet time-varying warm pixels are present in all IRS arrays, yet they are most problematic for Long-high and Long-low - the two Si:Sb arrays. In particular, Long-high spectra are most affected, since there are many more of these time-varying pixels, and the echelle orders cover a large fraction of the array. These pixels appear as "spikes" in the final, extracted one-dimensional spectra. While subtraction of campaign-based darks reduces the effect to some degree, much of the SINGS data were taken early in the

mission before the problem was fully appreciated, and darks were taken in earnest. We have made a careful attempt to remove residual warm pixels from the two-dimensional BCDs before spectral extraction, but observers are strongly encouraged to inspect the BCDs if spurious features (sharper than a single resolution element) are present in their spectra.

Wavelength Calibration Errors

The wavelength uncertainties in S11 have been measured by the SSC. At present the average wavelength uncertainties are less than 0.07μm in the low resolution data, and less than 0.01μm in the high resolution data[2].

Stray-Light Contamination

The SL array also contains two small "peak-up" (PU) fields which can lead to stray light contaminating the spectral orders. Present issues with the stray-light correction module employed in the pipeline can cause very faint horizontal bands of over or under correction in the BCD data. As a result, for SL order 1, we standardized on the *FLATAP* data which have not been corrected for stray light. Since SL1 is far from the PU fields, it should not suffer from stray-light contamination. For SL order 2, which is adjacent to the PU fields, we relied on stray-light-corrected BCD data for those galaxies with 1D model backgrounds subtracted (see Table 1), and FLATAP data otherwise.

Use of the Emission Line Maps

The emission line maps are most useful for assessing the spatial distribution of the line of interest. Accurate line fluxes should be obtained by measuring the line(s) from extracted 1D spectra of the region(s) of interest. Significant uncertainties of order 30-50% are expected for line intensities measured directly from the 2D maps.

5.5 Notes on Individual Galaxies

HolmbergII: No Short-Low data; for the Long-Low spectrum, a square extraction aperture has been employed. The infrared emission peaks 40” from the center of the LL strip.

Tol89: Brightest infrared source is located at the edge of the IRS maps, and is only barely visible in the LL, SL, and LH strips.

NGC5408: The infrared emission peaks 20” from the center of the IRS strips. The peak is absent from the SH and SL strips, and only a portion of it is present in the LH strip. A source external to NGC5408 appears in one of the SL outrigger fields.

[2] See the presentation by D. Shupe for the Spitzer Data Analysis workshop at this URL: http://ssc.spitzer.caltech.edu/ost/workshops/2005data/talks/shupe1.pdf

References

Reach, W., Morris, P, Boulanger, F and Okumura, K, Icarus, 164 (2003), pp. 384-403.

Sloan, G., Nerenberg, P. and Russell, M., IRS Technical Report 03001 (2003)

Table 2

Galaxy (a)	Type of background (b)
NGC 3773	Outrigger
NGC 3190	Outrigger
NGC 2798	Outrigger
NGC 4736	Model 1-D
NGC 4826	Outrigger
NGC 4725	Model 1-D
NGC 3049	Outrigger
NGC 2841	Model 1-D
NGC 7331	Dedicated
NGC 3627	Model 1-D
NGC 4579	Dedicated
NGC 3351	Dedicated
NGC 1566	Dedicated
NGC 3521	Model 1-D
NGC 5194	Model 1-D
NGC 2976	Model 1-D
NGC 3938	Model 1-D
NGC 7552	Outrigger
NGC 3198	Model 1-D
NGC 7793	Dedicated
NGC 0337	Outrigger
Tol 89	Outrigger
Ho II	
NGC 1705	Outrigger
NGC 5408	Outrigger

(a) Galaxies arranged according to Hubble type

(b) Different types of backgrounds as indicated in the text. Dedicated means sky observations obtained immediately following the mapping, Outrigger indicates sky background estimated from outer parts of a SL or LL map, Model-1D indicates an approximation to the background based on models and the observed 24mm flux.

6. Ancillary Data

6.1 Optical Imaging

Observations

Optical images for the galaxies in the SINGS sample were obtained at NOAO, as part of the Legacy Project, over the course of about 3 years (2001-2003). Observations were carried out at both the KPNO 2.1-m and the CTIO 1.5-m telescopes, using standard broad band B, V, R, and I filters, and a set of narrow-band filters in correspondence of the redshifted Hα line emission (0.6563 μm). For the 25 galaxies in the present delivery, the characteristics of the narrow-band filters (from the NOAO Web pages) are as follows:

Filter Name	Central Wavelength	FWHM	Peak Transmission
KP1468 (KPNO)	6567 A	84 A	72 %
KP1563 (KPNO)	6573 A	67 A	83 %
KP1390 (KPNO)	6587 A	72 A	67 %
KP1564 (KPNO)	6618 A	74 A	79 %
CT6568 (CTIO)	6568 A	19 A	70 %
CT6602 (CTIO)	6596 A	18 A	70 %

The 2Kx2K CCDs used for the observations have field-of-view (FOV) of 10' and 14.5', and pixel scale 0."305 and 0."433, at the KPNO-2.1-m and at the CTIO-1.5-m telescopes, respectively. Galaxies more extended than the CCD FOVs were imaged at multiple, overlapping pointings.

Exposure times ranged from 240 seconds to 1400 seconds (typically split into 2 separate exposures for cosmic ray removal.), in order to reach uniform depth of about 25 mag/arcsec^2 with signal-to-noise ratio of ~10 in the broad-band filters. Exposure times in the narrow-band filters were typically 1800 seconds, split into two separate exposures. In a minority of cases, a single narrow-band exposure was available.

Data Processing

Data reduction consisted of bias subtraction (using also the overscan region in the case of the KPNO images), flat-fielding (with both dome- and twilight-flats), single-image cosmic ray removal, and combination of pairs (or multiple) images at the same pointing/filter.

The southern 3' of the CCD FOV at the KPNO-2.1-m suffers from pronounced **vignetting**, whose intensity is pointing-dependent. We developed a

routine to remove as much as possible of the vignetting effect from each frame. The corrected frames were then used to create the final mosaics. See the section on `Known Problems' below for a quantification of the effectiveness of the vignetting-removal routine.

Astrometric solutions were derived for all optical images/mosaics, and the appropriate WCS keywords (FITS standard) stored in the image headers. All delivered optical images/mosaics have been rotated to the standard NE orientation.

Photometric and spectrophotometric standard stars were observed during each observing run to flux calibrate the images/mosaics. The spectrophotometric stars (e.g., Feige 34, HZ44) were used to obtain flux calibrations for the narrow-band filters. Effects of vignetting were negligible on the standard star frames, as the stars were usually centered on the CCD FOV, thus avoiding the vignetted edge.

Data Characteristics

All delivered optical images are in units of counts-per-seconds (CPS, stored in the UNITS keyword). The flux conversion keyword is PHOTFLAM, with units of Jy*sec/DN/pixel, as given by the keyword ZUNITS. Zeropoints are stored in the keyword ZPOINT (in Jy).

The images in this delivery are **not** background-subtracted. The narrow-band images (*_Hα.fits) generally contain emission from Hα, as well as the [NII](λλ 6548,6584), along with underlying stellar continuum. **Stellar continuum-subtracted narrow-band** images are also provided as *_Hα_sub.fits (this is the only optical image delivered for NGC5408, together with its rescaled continuum). Users can also construct their own pure emission-line images by scaling and subtracting the R-band images from the narrow-band images.

Most images have photometric accuracy within 5% (broad band) or 10% (narrow band). Care was taken to re-observe in photometric conditions any galaxy that had been previously acquired in non-photometric conditions. When this could not be accomplished (or there were larger-than-usual uncertainties in the standard stars calibrations) a COMMENT keyword was added to the image header. When more than one comment line is present, suffixes (COMMENT1, COMMENT2, etc.) are used.

In addition to astrometric and photometric keywords, the image headers contain other useful keywords detailing the observations (e.g., telescope, camera, filters, exposure times, etc.).

Conversion from count-rates to fluxes/magnitudes

Conversions from count-rates (CPS) to standard (Vega) magnitude scales for the optical images are accomplished with the following formula:

$$m = -2.5 * [\log(CPS*PHOTFLAM) - \log(ZPOINT)]$$

To convert continuum-subtracted narrow-band images from CPS to more familiar units for emission lines, e.g., erg s^{-1} cm^{-2}:

$$F(\text{erg } s^{-1} \text{ cm}^{-2}) = 3E\text{-}5 * CPS*PHOTFLAM*FWHM / CW^2$$

where FWHM and CW are the full-width half maximum and the central wavelength of the narrow-band filter, respectively. If the emission line(s) are shifted from the center of the filter's bandwidth, additional corrections for the filter's transmission curve need to be included in the above formula.

Known Problems

Comparison of the fluxes of stars in common between adjacent, overlapping pointings indicate that the vignetting-correction routine usually brings stellar fluxes into agreement within 2%-3%, but deviations as large as 5%-10% are not uncommon. Such residuals are often visible as `seams' at the overlapping points of adjacent frames.

Notes on individual galaxies:

NGC2798: residual fixed pattern noise present in all images. This is present in both unreduced and reduced images, and in the dark and bias frames as well.

NGC2976 and NGC3049: residual fixed pattern noise is present in the narrow-band images.

NGC3198: Marginal seeing conditions (broad PSF).

NGC3351 and NGC3521: BVI images for these galaxies are from the KPNO-4m plus MOSAIC Imager. The pixel scale is 0.27 arcsec/pixel. For NGC3351, no continuum-subtracted narrow-band image is delivered. The V-band image of NGC3521 shows a high-noise banding across the target.

NGC3773: Fixed pattern noise is present in the I and narrow band images.

NGC4725: Only the NE frame is available for the B band.

NGC4826: Optical images are from the SONG collaboration. The pixel scale is approximately 0.777 arcsec/pixel. The Hα image is already continuum-subtracted (information stored in the image header as COMMENT* keyword). A few bad columns (190-195) have been interpolated across, for the B, V, R, and I images. No calibration scales could be obtained for the R and I bands. No zeropoints available.

NGC5194: In addition to the nominal mosaics, a set of short-exposure mosaics are delivered for the V, R, and I bands, to aid treatment of the saturated nucleus of the galaxy. Residual vignetting is particularly noticeable in the R and I-band images of this galaxy, along the EW seam between the two overlapping pointings, and especially at the western side of the seam. In this latter region, the effect of

the residual vignetting translates into an 8% variation in the surface brightness of the galaxy across the seam, at a position located 174 arcsec west of the nucleus. The surface brightness at this location is about 360 times fainter than the nuclear one. The effects of residual vignetting become worse westward of this point, and quickly decrease in magnitude eastward of this point.

6.2 Optical Spectroscopy

Observations

Optical spectra for the SINGS galaxies in the wavelength range 0.36-0.70 μm, with resolution ~8 Angstrom, were obtained at the 2.3-meter Bok telescope with the B&C spectrograph, and at the 1.5-meter CTIO telescope with CSPEC.

Three types of long-slit spectra were obtained:

- Nuclear spectra: a 2".5 wide aperture (3" at CTIO) was pointed at the brightest central spot of the galaxy;
- 20" drift scans: the slit was drifted for 20" around the central region, while exposing;
- 55" drift scans: similar to the 20" drift scans, with a scan length of 55".

The data were taken during clear, photometric or semi-photometric conditions. A minimum of two sequential exposures were taken to facilitate cosmic-ray rejection. The total exposure times ranged from 600 seconds for the nuclear pointings to 900-2400 seconds for the 20" and 55" drift-scanned spectra. In the drift-scanned spectra the *effective* exposure time, t_effective, spent on a single spatial position of the galaxy is given by:

$$t\_effective = t\_exposure * (Aperture / Delta),$$

where t_exposure is the actual exposure time, Delta is the length of the scan in arcseconds (here, 20" or 55"), and Aperture is the slit width in arcseconds (here, 2.5" or 3"; see Kennicutt 1992, ApJS, 79, 255, for details).

Data Processing

The two-dimensional spectra were reduced with iSPEC2d, a customized longslit data reduction package developed in IDL by John Moustakas (UofA). The data were overscan- and bias-subtracted, trimmed, flat-fielded, and corrected for a low-order illumination pattern. The two-dimensional sky spectrum was subtracted from each

image before rebinning using the technique described in Kelson (2003, PASP, 115, 688). Sequential exposures were combined to reject cosmic rays; residual cosmic rays and hot pixels were flagged using LA_COSMIC (van Dokkum 2001, PASP, 113, 1420) and interpolated. The data were then wavelength- and flux-calibrated. Although standard stars were taken through good sky and seeing conditions, absolute spectrophotometric accuracy is not guaranteed, especially for the 2.5 arcsec nuclear spectra where slit losses from seeing may be significant. The relative spectrophotometric accuracy ranges from 1-4% based on the relative scatter in the derived sensitivity function. Two-dimensional error maps are generated using the known noise properties of the CCD and assuming Poisson statistics. These error maps are processed identically to the data.

One-dimensional data, error, and sky spectra were extracted in a 2.5" aperture for the nuclear spectra and a 20" aperture for the drift-scanned spectra using a low-order trace. A small wavelength shift was applied to the final wavelength solution by centroiding on the [O I] 5577 night sky line. The spectra have been de-reddened for foreground Galactic extinction assuming the O'Donnell (1994, ApJ, 422, 158) extinction curve and using the Schlegel, Finkbeiner, & Davis (1998, ApJ, 500, 525) reddening maps. The 20" drift-scan spectra accompany the equivalent-size extraction 1D IRS spectra.

Data Characteristics

The data are stored as ASCII files with the following columns:

1 – wavelength	[Angstrom]
2 – sky-subtracted data spectrum	[erg s^{-1} cm^{-2} A^{-1}]
3 - error spectrum	[erg s^{-1} cm^{-2} A^{-1}]
4 - sky spectrum	[erg s^{-1} cm^{-2} A^{-1}]

At the beginning of each file, basic information on the slit center is also reported.

The file names indicate the type of spectrum ("drift" or "nuclear"), the drift scan length, and the extraction aperture in arseconds. For example, in "ngc_0337_drift_020_020.txt", the first "020" is the scan-length while the second "020" is the aperture width. In "ngc_0337_nuclear_002.5.txt" only one number appears indicating the extraction aperture.

Notes on individual galaxies:

Ngc0337: Ill-defined nucleus, the tracing (placement of the extraction aperture's center) along the wavelength direction was not optimal.

NGC2976 and Tol89: only the central 20"x20" drift-scan spectrum is available.

HombergII, NGC5408, NGC7552: No spectra available for these galaxies.